

## Benzenoid links

Weiling Yang · Fuji Zhang · Douglas J. Klein

Received: 19 May 2009 / Accepted: 24 July 2009 / Published online: 15 August 2009  
© Springer Science+Business Media, LLC 2009

**Abstract** In this paper, we study new configurations of benzenoid hydrocarbons, called benzenoid links. Roughly speaking, a primitive corofusene is a closed narrow hexagonal ribbon with out-of-plane curvature 0. A primitive corofusene or the union of disjoint primitive corofusenes in  $\mathbb{R}^3$  is called a benzenoid link. In this paper, we determine the minimum number of hexagons needed for a nontrivial benzenoid link in different senses. We also determine the structures of the smallest and the second smallest nontrivial benzenoid links of different types and their numbers of Kekule structures. We list all the benzenoid Hopf links of type III with 22–25 hexagons by their canonical codes in the appendix.

**Keywords** Corofusenes · Benzenoid links · Hexagons · Benzenoid knots · Numbers of Kekule structures

---

Weiling Yang was supported in part by NSFC Grant 10501038. Fuji Zhang was supported in part by NSFC Grant 10671162. Douglas J. Klein was supported by the Welch Foundation of Houston, Texas, through grant BD-0894.

---

W. Yang · F. Zhang  
School of Mathematical Sciences, Xiamen University Xiamen, 361005 Fujian, China

W. Yang  
e-mail: ywlxmu@163.com

F. Zhang  
e-mail: fjzhang@xmu.edu.cn

D. J. Klein (✉)  
Texas A&M University at Galveston, Galveston, TX 77553-1675, USA  
e-mail: kleind@tamug.edu

## 1 Introduction

In the late nineteenth century physicists and mathematicians began to be interested in the study of knots. Since the 1970s, the research in this field has experienced explosive growth. One reason for this is due to the needs in mathematics and physics, with the early history described by Silver [1], and a thorough up-date of the modern developments in Kaufmann [2]. Another reason is that there occur knotted topological configurations of biomolecules, notably of DNA, as discovered [3] in the mid 1970s, but now with many more recent reviews [4,5], and also more recently the possibility of knotted proteins has gained [6,7] some attention. Indeed, chemists have had a continuing interest in the synthesis of non-trivial knotted molecules, as exemplified in the seminal 1961-paper of Frisch & Wasserman [8], and further there has been concern [9,10] that knotting & linking in polymers may notably effect their properties. A successful synthesis of a well characterized knotted molecule was reported [11] in 1989, though there were many early reports of probably linked “catenanes”, as recently reviewed [12]. Also in the solid state, multiply interlinked networks in crystals are recognizable [13] in an early (1941) article of Zhadanow [14], and also [15] in another compound in 1966. Now there are many reviews of knotted molecular structures [16–20]. The synthesis of the smallest molecular knots has become a challenging task for chemists. Also sometimes knot theory has been proposed [21,22] as of use in the characterization of other (unknotted) molecular structures.

On the other hand, the study of benzenoid hydrocarbons has a long history. The pioneering synthetic effort and key successes can be found in the excellent references [23–29]. More than 20 years ago, a primitive coronoid was successfully synthesized by Diederich and Staab after 10 years of effort [see Fig. 1a]. The physical and chemical properties had also been studied by chemists [30–35]. The second primitive coronoid was synthesized 8 years after the synthesis of the first one [see Fig. 1b]. Some theoretical studies were carried out, including molecular geometry, aromaticity, magnetic susceptibility, H-chemical shifts and zero-field splitting [36–46]. Then, two books [47,48] on the theory of coronoid hydrocarbons were published in Lecture Notes in Chemistry (Vol. 54 and Vol. 62). It is natural to consider the primitive coronoids as molecular realization of the trivial knots. Another existing hydrocarbon molecular structures that consist of hexagons, and are termed helicenic systems (cf. Fig. 1c, [46,49–55]). This type of benzenoid hydrocarbon is geometrically nonplanar. The

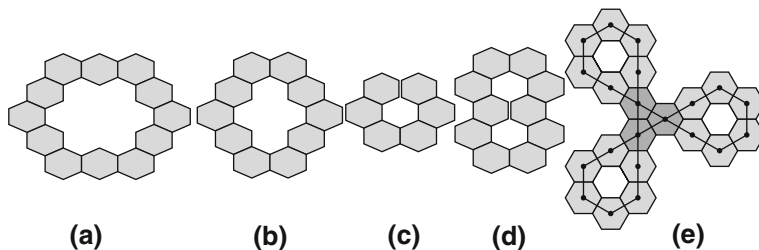
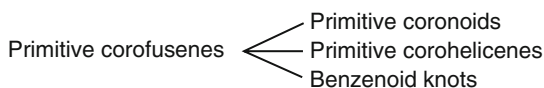


**Fig. 1** **a, b** The first two synthesized primitive coronoids. **c** A synthesized hexahelicene (more helicenes are indicated in Fig. 2 by their inner dual graphs). **d, e** Primitive corohelicenes

structures of primitive coronoid systems and helicenes inspire us to consider the structures (geometrically planar and nonplanar) of closed benzenoid chains with curvature 0, called primitive corofusenes. Note that a primitive corofusene formed by a closed narrow hexagonal-ring ribbon with curvature 0 can be considered as a knot made from a hexagonal chain. The criterion of 0-curvature [56] can be interpreted to mean that the hexagons in the chain are very nearly regular, and successive rings are very nearly co-planar. Now we define the inner dual graph of a primitive corofusene in the following way: a vertex is drawn at the center of each hexagon, and two vertices are connected by a straight line segment if they lie in adjacent hexagons. One can see that the inner dual graph of a primitive corofusene is a polygonal knot, i.e., a knot that is made by connecting a finite set of straight line segments in  $R^3$  through their end points. A primitive corohelicene is a geometrically nonplanar primitive corofusene whose inner dual graph is a trivial polygonal knot. It is natural to consider the geometrically nonplanar primitive corofusene whose inner dual graph forms a nontrivial polygonal knot. Thus the primitive corofusenes with inner dual graph homeomorphic to a circle in  $\mathbb{R}^3$  can be classified as the following types (cf. [48] P. 45).



A primitive coronoid is a geometrically planar primitive corofusene. (eg Fig. 1 (a))

A primitive corohelicene is a geometrically nonplanar primitive corofusene whose inner dual graph is a trivial polygonal knot. (eg Fig. 1 (d,e))

A benzenoid knot is a geometrically nonplanar primitive corofusene whose inner dual graph is a nontrivial polygonal knot. (eg Fig. 6)

In this paper, we mainly study the new configurations of benzenoid hydrocarbons, called benzenoid links, each of which is a primitive corofusene or a finite union of disjoint corofusenes in  $\mathbb{R}^3$ . We determine the minimum number of hexagons needed for a nontrivial benzenoid link in different cases. We also determine the structures of the smallest and the second smallest nontrivial benzenoid links in each case and their numbers of Kekule structures. We list all the benzenoid Hopf links of type III with 22–25 hexagons by their canonical codes in the appendix.

## 2 Preliminaries

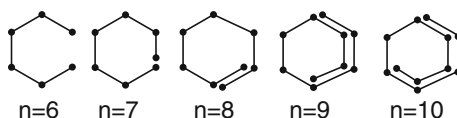
A graph  $G$  is an ordered triple  $(V(G), E(G), \psi_G)$  consisting of a non-empty set  $V(G)$  of vertices, a set  $E(G)$ , disjoint from  $V(G)$ , of edges, and an incidence function  $\psi_G$  that associates each edge of  $G$  with an unordered pair of (not necessarily distinct) vertices of  $G$ . A walk in  $G$  is a finite non-null sequence  $W = v_0 e_1 v_1 e_2 v_2 \cdots e_k v_k$ , whose terms are alternately vertices and edges, such that, for  $1 \leq i \leq k$ , the ends of  $e_i$  are  $v_{i-1}$  and  $v_i$ . If the edges  $e_1, e_2, \dots, e_k$  of a walk  $W$  are distinct,  $W$  is called a trail. If, in addition, the vertices  $v_0, v_1, \dots, v_k$  are distinct,  $W$  is called a path. A chain in  $G$  is a path whose internal vertices (if there are any) all have degree two in  $G$ . A chain is called a maximal chain in  $G$  if its initial and terminal vertices both have degree greater than two in  $G$ . A link with  $n$  components is a subset of Euclidean space

$E_3$  such as to consist of  $n$  disjoint non-self-intersecting cyclic curves. A knot or cycle is a link with a single component.

Links are to be correlated with suitable benzenoid-like constructions. A (finite) benzenoid  $B$  is a collection of all the 6-cycles inside a simple closed (Jordan) curve  $C$  in the honeycomb network with  $C$  marking the boundary of the 6-cycle region constituting  $B$ . If inside such a  $B$  one deletes subsets of internal edges such that every remaining edge occurs in one or more of the remaining 6-cycles, then one obtains a multi-coronoid (though when there is just one resultant hole introduced, it is often termed just a coronoid). These benzenoids & multi-coronoids may be viewed to be constructed from geometrically regular hexagons with co-planar fusions at single edges, so that all is embedded in the Euclidean plane  $\mathbb{R}^2$ . A more general construction utilizes essentially regular (or more briefly e-regular) hexagons which mathematically are arbitrarily close to being regular such as to allow the same local structures already utilized for benzenoids and multi-coronoids but now allowing embeddings in Euclidean space  $\mathbb{R}^3$ . That is, fusions of e-regular hexagons occur along edges such that each site has no more than three edges incident, no more than two hexagons fuse at a given edge, and adjacent hexagons are e-co-planar, in the sense that they are mathematically arbitrarily near to being co-planar. More specifically these “essentiality” or “e” conditions are that the sites involved are viewable as all being within an arbitrarily small  $\varepsilon > 0$  distance of corresponding sets of sites which are exactly regular or co-planar. Were one to take the limit  $\varepsilon \rightarrow 0$ , non-disjointness could result in general. With such a restriction there is in an idealized mathematical model with arbitrarily little curvature out of the plane, and one may say the net (combinatorial) curvature is 0. This then allows the “helicenic” structures of Fig. 1c,d as well as further helicenes of 7 or more rings, with full rings “overlapping” one another. Notably such  $n$ -ring helicenes are experimentally known for  $n$  up to at least 10 (see Fig. 2). The enumeration of helicenes are reported in [50]. All this may also be viewed in terms of multiple sheets of the regular honeycomb lattice, with shifts from one sheet to another taken to avoid self-intersection. Now granted such a polyhex (or generalized benzenoid)  $G$  embedded in  $E_3$ , one may associate an inner dual  $G^*$  with vertices at centers of the hexagonal faces and edges between such vertices at the centers of adjacent (edge-fused) faces. If the resultant inner dual  $G^*$  is a link, then  $G^*$  is said to be a polygonal link, and  $G$  is a benzenoid link.

There are some general aspects of these benzenoid links [56–59]. First, each component of such a  $G^*$  is a cycle  $C$ , and the corresponding component  $C^{(*)}$  of  $G$  is a cyclo-phenacene [56–58]. If such a component of  $G^*$  contains  $n$  sites, then the corresponding component is a cyclo- $n$ -phenacene, with a formula  $C_{4n}H_{2n}$ , since every hexagon in such a cycle is seen to have two degree-2 sites (with an H atom attached). Now further each such cycle  $C$  has a writhe number  $W(C)$ , which is the number of full rotations through which one turns in following the edges of  $C$  around  $C$  to return to the initial site. Moreover, the associated cyclo-phenacene  $C^{(*)}$  has two boundaries,

**Fig. 2** The inner dual graphs of 6, 7, 8, 9, 10-ring helicenes



since the essentiality conditions mean that it is not like a Mobius strip. Moreover the number of H-atoms (equal to the number of degree-2 sites) on either of these boundaries depends on the writhe number in a fairly simple way: the number of H atoms on the two boundaries is  $n + 6W(C)$  &  $n - 6W(C)$ , whence (if  $W(C) \neq 0$ ) we call the two respective boundaries the *outer* & the *inner*. To see this result note that as one proceeds around a boundary of  $C^{(*)}$  one turns through a net angle of  $W(C) \times 360^\circ$ , with each turn at a site being  $\pm 60^\circ$ , and note that the  $\pm$  sign occurs at a degree-2 or degree-3 site, with this correspondence being opposite for the two boundaries of  $C^{(*)}$ . (This result generalizes the well-known result for benzenoids that the number of H atoms on the outer boundary is six more than the number of degree-3 sites on the boundary - and it generalizes a similar result for multi-coronoids, involving 6 more for the outer boundary and six less for the boundary of each hole). For a  $C^{(*)}$  with  $W(C) = 0$ , there evidently is an ambiguity as to which boundaries of  $C^{(*)}$  one would wish to call *inner* & *outer*.

*Remark 1* There is an interesting article [60] which considers polyphenylenes. It is not difficult to see that the polyphenylene can also form links. We will discuss them elsewhere.

A benzenoid link  $G$  and its inner dual graph  $G^*$  may be projected into the Euclidean plane. That is, each hexagon of  $G$  is taken to be a hexagon of the regular honeycomb lattice such that neighbor hexagons are preserved, whence at most two hexagons of  $G$  can be mapped to the same hexagon of the honeycomb lattice. Also the inner dual graph  $G^*$  is similarly mapped to  $E_2$ , with the vertices  $G^*$  mapped to the centers of the corresponding image hexagons in the honeycomb lattice. The resultant structure  $S(G^*)$  is termed the shadow of the benzenoid link  $G$ .

The unit of length is conveniently taken to be that of the edges in the underlying honeycomb lattice. Further we consider subclasses of all benzenoid links  $G$  which satisfy different sets of further conditions, which basically demand a minimal amount of “overlapping” while still allowing non-trivial knotting:

- (i) The length of any maximal chain of  $S(G^*)$  is at least 2.
- (ii) There is at least one hexagon of  $G$  in the interior of every face of  $S(G^*)$  (say a hole of the face).
- (iii) The Euclidean distance between any nonadjacent vertices is greater than 1, except the two nonadjacent vertices are both adjacent to the same vertex of degree 4 (e.g. see u, v, w in Fig. 2).
- (iv) Edge crossings of  $G^*$  are “straight”, in the sense that for any degree-4 vertex w of  $S(G^*)$  the associated incident edges form a cross, as in Fig. 3, with opposite edges corresponding to adjacent edges of  $G^*$  (Fig. 4).

The examples in Fig. 5 are chosen to indicate that the conditions (ii), (iii), (iv) are independent, in the sense that there exist examples (see Fig. 5a–c) which violate one condition, while not violating the other two. On the other hand, if the condition (i) is violated, at least one of the conditions (ii), (iii), (iv) is violated, since there is only three ways to produce a maximal chain with length 1 (see Fig. 5d–f).

If all four conditions are satisfied, then  $G$  is said to be a benzenoid link of type I; while if the first three are satisfied, then  $G$  is said to be of type II; if only the first

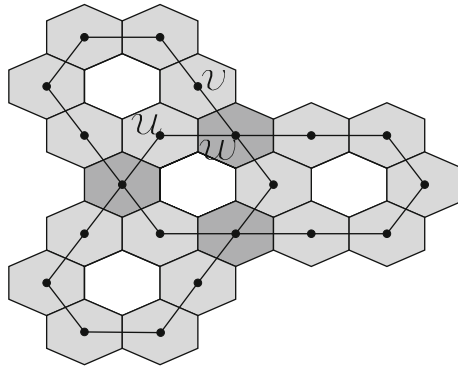


**Fig. 3** The shadow of a benzenoid trefoil knot

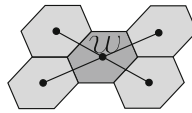


**Fig. 4** Two edges cross "straightly"

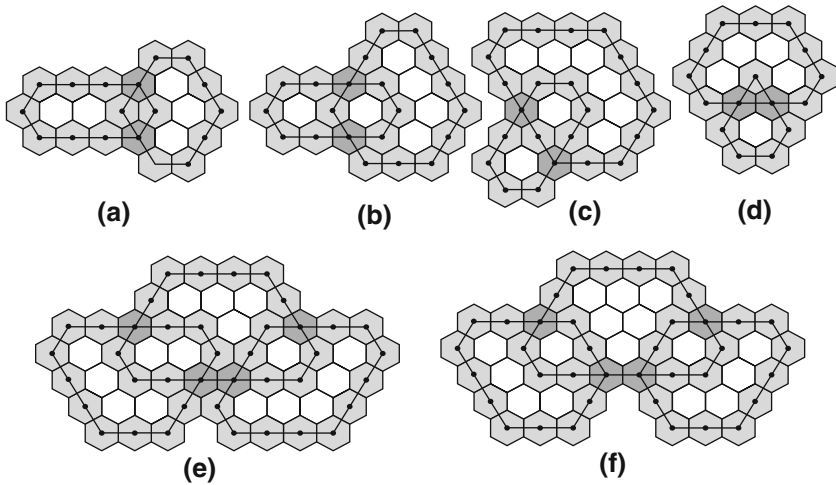


**Fig. 5** **a–c** Violate conditions (ii), (iii), (iv) respectively. **d–f** Violate condition (i) and conditions (ii), (iii), (iv) respectively

two condition is satisfied, then  $G$  is said to be of type III; In the next section, we will consider the three types of benzenoid links respectively.

These conditions may be viewed first to correlate more closely with typical topological definitions for knots not correlated to a discrete underlying lattice. On the chemical side, bearing in mind the configuration of synthesised coronoids these conditions are likely to be satisfied for all benzenoid links, Though it is just this smaller sized knots focused on here.

*Remark 2* If we suppress all the vertices of degree 2 of the shadow  $S(G^*)$ , we will get a reduced shadow. This is 4-regular, and it can be regarded as a universe of the corresponding link diagrams.

*Remark 3* Condition (ii) implies that every face of  $S(G^*)$  has at least 6 vertices.

*Example 1* Two benzenoid trefoil knots and two benzenoid Hopf links of type I, II and III (Fig. 6).

### 3 Main results

Let  $H(L)$  denote the number of hexagons for a benzenoid link  $L$ . We get:

**Theorem 3.1** *For any nontrivial benzenoid link  $L$  of type I,  $H(L) \geq 24$ . Moreover, equality holds if and only if  $L$  is one of the four benzenoid links in Fig. 6.*

*Proof* Throughout this proof, a benzenoid link is understood to be a benzenoid link of type I. Clearly there exists a nontrivial benzenoid link  $L_0$ , such that for any nontrivial benzenoid link  $L$ ,  $H(L_0) \leq H(L)$ . All we need to prove is that  $L_0$  is either a benzenoid trefoil knot or a benzenoid Hopf link, and any benzenoid trefoil knot or benzenoid Hopf link different from the ones in Fig. 6 has more than 24 hexagons. From Example 1, we immediately know  $H(L_0) \leq 24$ . We identify the embedding of  $L_0$  in the planar hexagonal lattice with the reduced shadow  $G$ , and identify the benzenoid link with its inner dual graph. Consider the boundary  $C$  of the infinite face of  $G$ . Obviously,  $C$  is a closed trail.

Claim 1: The vertices of  $C$  are distinct. That is,  $C$  is a cycle.

Otherwise,  $G$  has a configuration as Fig. 7. we can take  $G$  apart as in Fig. 7. Then the link corresponding to  $G$ , denoted  $L_0$ , is the connected sum of the links corresponding to  $A$  and  $B$ . Since  $L_0$  is nontrivial, one of the links corresponding to  $A$  and  $B$  is nontrivial. Choose the nontrivial one. There are at least six fewer hexagons in the corresponding benzenoid link induced by  $L_0$  than  $L_0$ , a contradiction.

Claim 2: All the vertices of  $G$  are on the cycle  $C$ .

Color the faces of  $G$  with black and white properly, such that the infinite face is colored white. If there is a vertex inside  $C$ , near the vertex there are two white regions  $A, B$  contained entirely in  $C$ . Let  $C_A, C_B$  denote the boundaries of  $A, B$  respectively. Considering positions of  $A$  and  $B$ , there are exactly two cases as shown in Fig. 8.

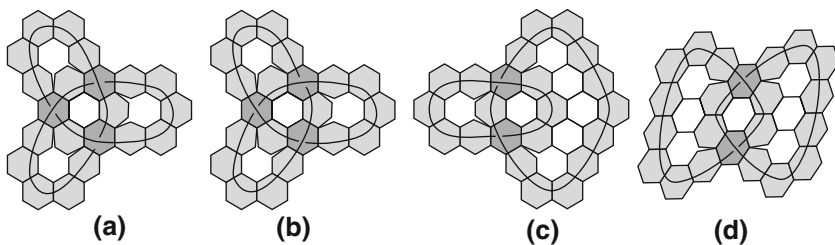


**Fig. 6** Two benzenoid trefoil knot and two benzenoid Hopf links with 24 hexagons

**Fig. 7** Decomposition of  $G$  into  $A$  &  $B$

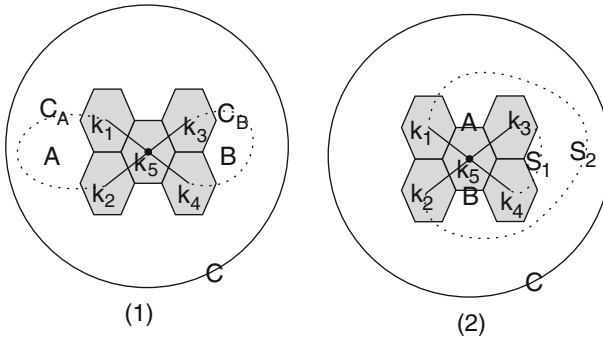
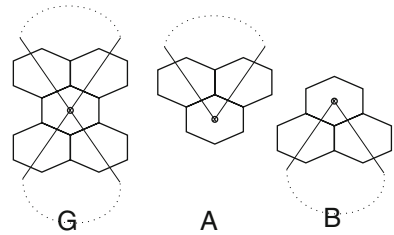


**Fig. 8** (1):  $A, B$  are distinct regions. (2):  $A, B$  are the same region, and  $S_1 \cup S_2 = C_A = C_B$

Although  $C$  and  $C_A \cup C_B$  can have common vertices, they cannot have common edges (because  $A, B$  and the infinite face are all colored white). Furthermore the common vertex corresponds to multilayer hexagons.

Clearly, in either of the two cases, there are at least three faces in  $C$ . There are at least three hole hexagons by condition (ii). Note that these hole hexagons are different from  $k_1, k_2, k_3, k_4, k_5$ . By condition (i),  $k_1, k_2, k_3, k_4, k_5$  and two other hexagons on  $C_A \cup C_B$  are not on  $C$ . That is, they are contained entirely in  $C$ . Then there are at least  $3 + 5 + 2 = 10$  hexagons contained entirely in  $C$ . A benzenoid cycle with less than 14 hexagons cannot contain greater than 8 hexagons inside (cf. [47] P94, 95). So  $C$  has at least 14 hexagons. On the other hand,  $|C_A| + |C_B| \geq 6 + 6 = 12$  and  $|S_1| + |S_2| \geq 6 + 6 = 12$  by Remark 3. So the benzenoid link  $L_0$  has at least  $14 + 12 = 26$  hexagons in either case, a contradiction.

Claim 3: Let  $C = v_0v_1 \dots v_n(v_n = v_0)$ , then for any edge  $v_iv_j \in E(G)$ ,  $\min\{|i - j|, n - |i - j|\} = 1$ .

Suppose, to the contrary, that there exist  $i$  and  $j$  such that  $\min\{|i - j|, n - |i - j|\} \geq 2$  and  $v_iv_j \in E(G)$ . Since  $G$  is 4-regular, there exist  $v_s$  and  $v_t$  such that  $v_iv_s, v_iv_t \in E(G)$ . Without loss of generality, we assume that  $s \in \{i, i + 1, \dots, j\} \pmod n$ . Then  $t \in \{i, i + 1, \dots, j\} \pmod n$ . Otherwise, since  $G$  would be planar and 4-regular,  $G - \{v_{j+1}, v_{j+2}, \dots, v_{i-1}\} \pmod n$  is a graph containing only one vertex  $i$  with odd degree. This is impossible. Then  $C$  has the following configuration (Fig. 9):

The line  $l$  intersects  $C$  at two points, and takes  $C$  apart. Clearly,  $L_0$  is the connected sum of the links corresponding to  $A \cup \{v_kv_{k+1} | k = i - 1, i, \dots, j \pmod n\}$  and  $B \cup \{v_kv_{k+1} | k = j, j + 1, \dots, i - 1 \pmod n\}$ , where  $A$  is the induced subgraph of  $\{v_{j+1}, v_{j+2}, \dots, v_{i-1}\} \pmod n$  and  $B$  is the induced subgraph of  $\{v_i, v_{i+1}, \dots, v_j\}$



**Fig. 9** The long vertical line partitions the graph into  $A$  and  $B$

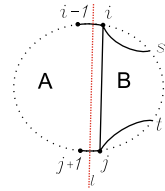


**Fig. 10**  $G$

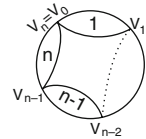
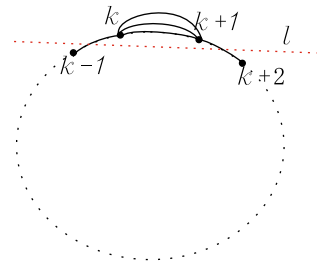


**Fig. 11**  $G$



(mod  $n$ ). Note that both  $A$  and  $B$  are non-empty. Since  $L_0$  is nontrivial, one of the links corresponding to  $A \cup \{v_k v_{k+1} | k = i-1, i, \dots, j \pmod n\}$  and  $B \cup \{v_k v_{k+1} | k = j, j+1, \dots, i-1 \pmod n\}$  is nontrivial. Choose the nontrivial one. There are at least six fewer hexagons in the corresponding benzenoid link induced by  $L_0$  than in  $L_0$ , a contradiction.

Claim 4:  $G$  has the form of Fig. 10.

From Claim 3, we know that if  $av_i \in E(G)$ , then  $a = v_{i+1}$  or  $a = v_{i-1}$ , for any  $i$ .  $G$  is 4-regular, then  $G$  has the form of Fig. 10. Otherwise there exist  $k$  ( $k = 0, 1, \dots, n-1$ ) and  $n > 2$  such that  $v_k$  is adjacent to  $v_{k+1}$  with three different edges (see Fig. 11).

By the reason mentioned in Claim 3, there exists a nontrivial benzenoid link with at least 6 hexagons fewer than  $L_0$ , a contradiction.

Claim 5:  $n \leq 3$ .

Case 1:  $n \geq 5$ . There exist  $n$  edge-disjoint cycles in  $G$  and each cycle has only a single hexagon in common with the next (see Fig. 10). Furthermore, the common hexagon is of multi-layers. Every cycle has at least 6 hexagons. So the benzenoid link has at least  $6n \geq 30$  hexagons, a contradiction.

Case 2:  $n = 4$ . By the reason mentioned above, this benzenoid link has at least 24 hexagons. Furthermore, when it has exactly 24, each of the four cycles has exactly 6 hexagons. Figure 12 shows all the cases of the embedding of three cycles, such that each of the cycles has exactly 6 hexagons. Obviously, adding one more cycle with 6 hexagons cannot get  $C = v_0 v_1 v_2 v_3$ . So this benzenoid link has more than 24 hexagons, a contradiction.

Claim 6:  $L_0$  is either a benzenoid trefoil knot or a benzenoid Hopf link.

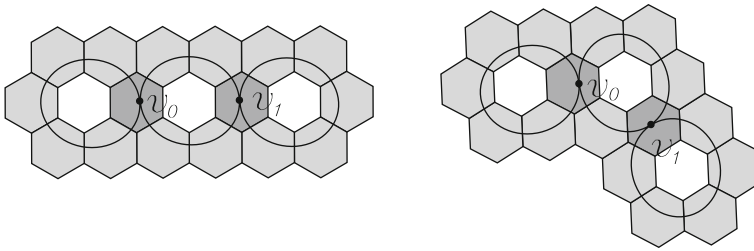


**Fig. 12** Embeddings of 3 cycle

It is easy to check the following: if  $n = 3$ , the corresponding benzenoid link is either a benzenoid trefoil knot or a trivial benzenoid knot; if  $n = 2$ , the corresponding benzenoid link is either a benzenoid Hopf link or a trivial benzenoid link.

Now we turn to show that any benzenoid trefoil knot or benzenoid Hopf link different from the ones in Fig. 4 has greater than 24 hexagons.

The shadow of each component of a benzenoid Hopf link is a primitive coronoid. So the shadow of a benzenoid Hopf link can be regarded as a union of two primitive coronoids, such that it satisfies the four conditions and its inner dual graph is the shadow of a benzenoid Hopf link. All the primitive coronoids with less than 16 hexagons were listed in [47] P94–97. With careful checking, we get that the minimum possible numbers of hexagons for a benzenoid Hopf link is 24 and any benzenoid Hopf link different from the ones in Fig. 6 has greater than 24 hexagons.

If the hexagons near one of the three inner-dual vertices of the shadow of a benzenoid trefoil knot take the form of Fig. 13 (1). After removing the vertex [see Fig. 13.(3)] it becomes a benzenoid Hopf link. Note that when removing this vertex, in fact we remove two hexagons (one is beneath the other). So the original benzenoid trefoil knot has at least  $24 + 2 = 26$  hexagons. If the hexagons near every vertex take the form of Fig. 13(2), we remove all of the three vertices with degree 4 as in Fig. 13(3). Then we get a trivial benzenoid link with three components. We have mentioned that a benzenoid cycle has at least 6 hexagons. So the original benzenoid trefoil knot has at least  $6 \times 3 + 2 \times 3 = 24$  hexagons. When we get the minimum number 24, the benzenoid trefoil knot is constructed by three benzenoid cycles with 6 hexagons, and each cycle connects with the next by a crossing. It is easy to check that only the two

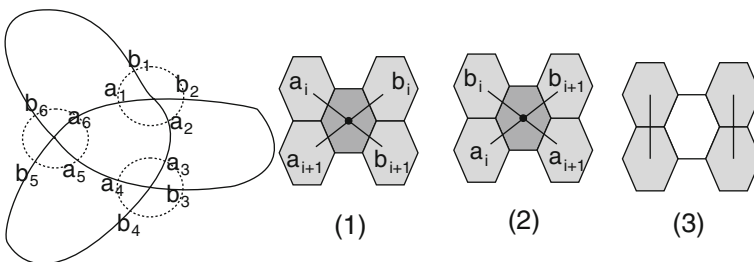


**Fig. 13** The hexagons near each of inner-dual vertices of the shadow take the form of (1) or (2)

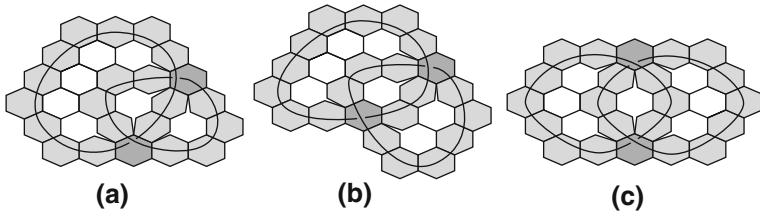


Fig. 14 Some benzenoid links of type II with 24 hexagons

benzenoid trefoil knot in Fig. 6 can satisfy these conditions. Thus we have completed the proof of the theorem.  $\square$

Next, we consider benzenoid links  $L$  of type II. It seems to be reasonable to think that the minimum number of hexagons of the benzenoid links of type II is smaller than 24. But this is not so. In the following theorem, we show that the minimum number of hexagons of the benzenoid links of type II is equal to that of type I, but there are three more benzenoid links with the minimum number of hexagons (Fig. 14).

**Theorem 3.2** *For any nontrivial benzenoid link  $L$  of type II,  $H(L) \geq 24$ . Moreover, equality holds if and only if  $L$  is a benzenoid link in Figs. 6 or 14.*

*Proof* A benzenoid link is understood to be of type II throughout this proof. There is a striking similarity between the proofs of Theorem 3.1 and 3.2. We only need to make a slight change to prove the fact that any benzenoid trefoil knot or benzenoid Hopf link different from the ones in Figs. 6 and 14 has more than 24 hexagons.

The shadow of a benzenoid Hopf link can be regarded as a union of two primitive coronoids, such that it satisfies the first three conditions and the inner dual graph of it is the shadow of a benzenoid Hopf link. With a careful check, we find that the minimum possible hexagons for a benzenoid Hopf link is 24 and any benzenoid Hopf link different from the ones in Figs. 6 and 14 has greater than 24 hexagons.

Now we turn to the benzenoid trefoil knots. Figure 15 lists all the possible cases of  $a_i, b_i$  ( $i = 1, 2, \dots, 6$ ) near the vertices (cf. Fig. 13). If the hexagons near one of the three vertices take the form of Fig. 15(2), (3), (4), (5), (6) or (7), we can find a benzenoid Hopf link, such that the benzenoid Hopf link has fewer hexagons than the original benzenoid trefoil knot.

We take Fig. 15(7) as an example. By condition (iii),  $A, B, C, D, E$  (see Fig. 16a) are not on any edges of the shadow. So  $b_i$  and  $F, b_{i+1}$  and  $G$  are consecutive hexagons on some edges of the shadow. Then  $H$  ( $I$ , resp.) is either a successive hexagon to

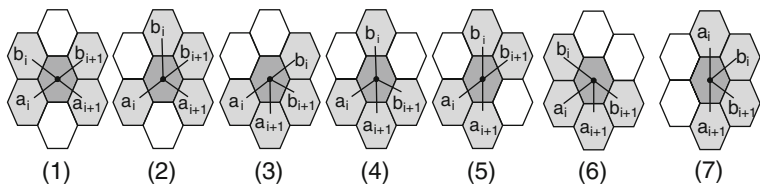
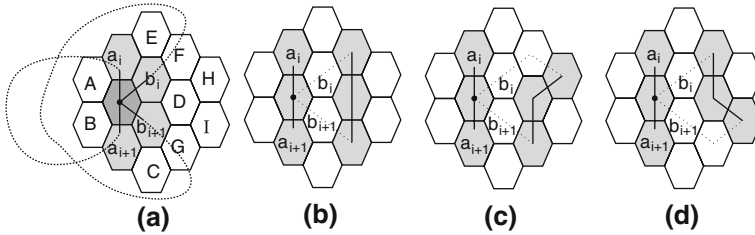


Fig. 15 The hexagons near vertex takes the form of (1), (2), (3), (4), (5), (6), or (7)



**Fig. 16** One case

$F$  ( $G$ , resp.), or on none of the edges of the shadow. If  $H$  and  $I$  are not on any edges, we remove  $b_i, b_{i+1}$  as Fig. 16b. If  $H$  is successive to  $F$  and  $I$  is not on any edge of the shadow, we have as Fig. 16c. If  $I$  is successive to  $G$  and  $H$  is not on any edge of the shadow, we have as Fig. 16d. By condition (iii), it is not possible that  $H$  and  $I$  are successive hexagons to  $F$  and  $G$ , respectively. Then we get a benzenoid Hopf link which has less hexagons than the original benzenoid knot. So the original benzenoid trefoil knot has more than 24 hexagons. Other cases can be considered similarly. If all the vertices take the form of Fig. 15(1), then as in the proof of Theorem 3.1, only the two benzenoid trefoil knot in Fig. 6 have 24 hexagons. Thus we have proved the theorem.  $\square$

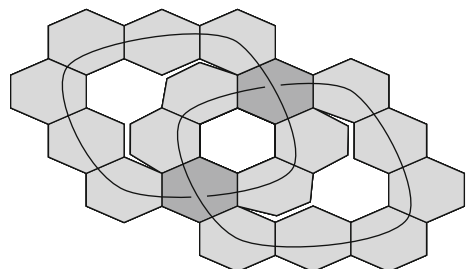
Now we turn to the case of type III. Obviously, any benzenoid link of type I or type II is a benzenoid link of type III, but the converse is not true.

**Theorem 3.3** *For any nontrivial benzenoid link  $L$  of type III,  $H(L) \geq 20$ . Moreover, equality holds if and only if  $L$  is the benzenoid link in Fig. 17.*

*Proof* A benzenoid link is understood to be of type III throughout this proof. Choose  $L_0$  as in Theorem 3.1. From Fig. 17,  $H(L_0) \leq 20$ . The proof that  $L_0$  is either a benzenoid trefoil knot or a benzenoid Hopf link is the same as the proof in Theorem 3.1 and 3.2. To complete the proof, we only need to show that any benzenoid Hopf link different from the one in Fig. 17 has more than 20 hexagons, and any benzenoid trefoil knot has more than 20 hexagons.

The shadow of a benzenoid Hopf link can be regarded as a union of two primitive coronoids, such that it satisfies the first two conditions and the inner dual graph of it is the shadow of a benzenoid Hopf link. With careful checking, we get that the minimum

**Fig. 17** The benzenoid Hopf link with 20 hexagons that is of type III, but not type I or II



possible numbers of hexagons for a benzenoid Hopf link is 20 and any benzenoid Hopf link different from the ones in Fig. 17 has greater than 20 hexagons.

By condition (i), (ii), the thin line (thick, resp.) in Fig. 18 contains at least 5 (3, resp.) hexagons inside. And they are similar to primitive coronoids. By [47] P94–97, we know the thin (thick, resp.) line has at least 11 (10, resp.) hexagons. Moreover there cannot exist a benzenoid trefoil knot with the thin line having 11 hexagons. So any benzenoid trefoil knot has at least 22 hexagons. This completes the proof. □

Now we list all the benzenoid links of type I, II with 25 hexagons, and the benzenoid links of type III with 21 hexagons. Instead of giving a complete proof here, we just point out that it is based on the following facts:

- (1) For any second smallest nontrivial benzenoid link of type I or II, Claims 1–5 hold. Note that in Fig. 12, adding one more cycle with 7 hexagons cannot get  $C = v_0v_1v_2v_3$ . So any second smallest nontrivial benzenoid link of type I or II is a Hopf benzenoid link or a trefoil benzenoid knot.
- (2) By condition (i) and (ii), each component of a benzenoid Hopf link of type I, II or III contains at least 3 hexagons inside. Then each component of a benzenoid Hopf link of type I, II or III with 25 hexagons has more than 9 hexagons and less than 16 hexagons. So from [47] P94 – 97, we can get all the benzenoid Hopf links of type I, II or III with 25 hexagons.
- (3) When we induce a benzenoid Hopf link from a benzenoid trefoil knot as in the proof of Theorems 3.1 and 3.2, we remove at least two hexagons. So there cannot exist a benzenoid trefoil knot of type I or II with 25 hexagons.
- (4) From the proof of Theorem 3.3, there cannot exist any benzenoid trefoil knot with 21 hexagons.
  1. All the benzenoid links of type I with 25 hexagons are listed in Fig. 19.
  2. All the benzenoid links of type II with 25 hexagons are listed in Figs. 19 and 20.
  3. All the benzenoid links of type III with 21 hexagons are listed in Fig. 21.

**Fig. 18** The inner dual graph of benzenoid trefoil knot

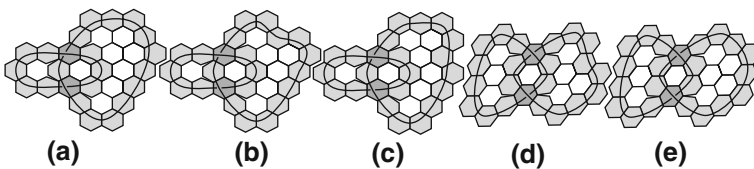
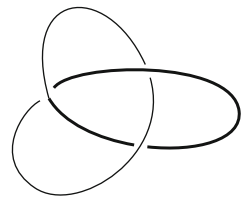


**Fig. 19** Benzenoid Hopf links of type I and II with 25 hexagons

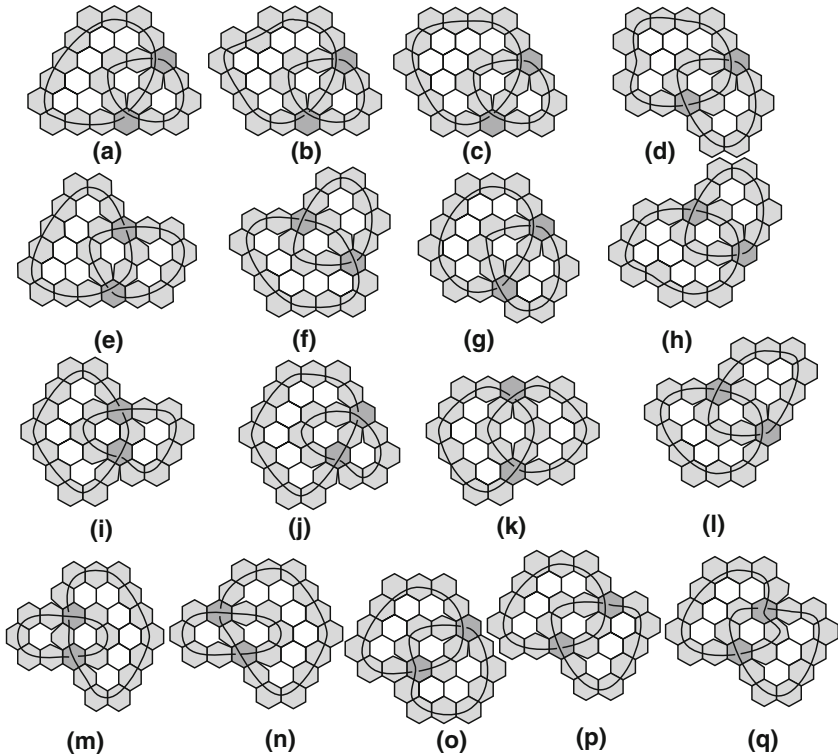


**Fig. 20** Benzenoid Hopf links of type II with 25 hexagons

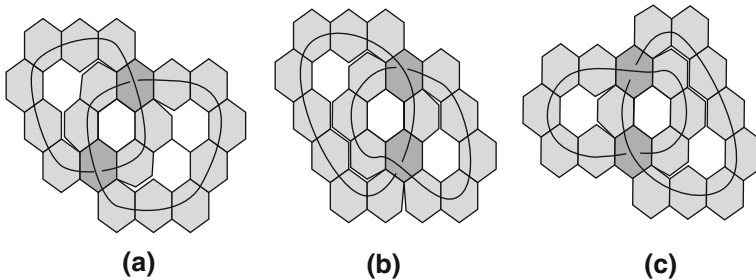


**Fig. 21** Benzenoid Hopf links of type III with 21 hexagons

*Remark 4* The Kekule structures play an important role in the study of stability for an aromatic system [25]. By the approach of recurrence relations [25] or the approach of transfer matrixes [56], we can get the numbers of Kekule structures of the benzenoid trefoil knots in Fig. 6. [47] P94–97 also list the numbers of Kekule structures of the primitive coronoids with less than 16 hexagons. By Fact (2), we can get the numbers of Kekule structures of any benzenoid Hopf link with less than 26 hexagons.

We summarize our now obtained smaller benzenoid links  $B$ , along with their computed Kekule structure counts  $K(B)$  in Table 1.

**Table 1** The numbers of Kekule structures of the benzenoid links in Figs. 6, 14, 17, 19–21

<i>B</i>	<i>K</i> ( <i>B</i> )	<i>B</i>	<i>K</i> ( <i>B</i> )	<i>B</i>	<i>K</i> ( <i>B</i> )
Fig. 6a	19604	Fig. 6b	19604	Fig. 6c	$68 \times 260$
Fig. 6d	$112 \times 112$	Fig. 14a	$85 \times 365$	Fig. 14b	$108 \times 224$
Fig. 14c	$200 \times 200$	Fig. 17	$85 \times 85$	Fig. 19a	$68 \times 380$
Fig. 19b	$68 \times 416$	Fig. 19c	$68 \times 512$	Fig. 19d	$112 \times 252$
Fig. 19e	$112 \times 224$	Fig. 20a	$85 \times 380$	Fig. 20b	$85 \times 608$
Fig. 20c	$85 \times 490$	Fig. 20d	$108 \times 404$	Fig. 20e	$108 \times 224$
Fig. 20f	$108 \times 260$	Fig. 20g	$108 \times 365$	Fig. 20h	$108 \times 461$
Fig. 20i	$128 \times 260$	Fig. 20j	$104 \times 380$	Fig. 20k	$200 \times 224$
Fig. 20l	$148 \times 224$	Fig. 20m	$68 \times 512$	Fig. 20n	$68 \times 380$
Fig. 20o	$229 \times 224$	Fig. 20p	$112 \times 224$	Fig. 20q	$112 \times 252$
Fig. 21a	$85 \times 108$	Fig. 21b	$104 \times 108$	Fig. 21c	$68 \times 108$

**Acknowledgments** FZ acknowledges P.W. Fowler for his helpful discussion in Ilmenau. DJK acknowledges the support of the Welch Foundation of Houston, Texas, through grant BD-0894. We would like to thank professor Z. Chen and Dr. Xian'an Jin for their helpful comments.

### Appendix

In this appendix, we list all the canonical codes of the benzenoid Hopf links of type III with 22–25 hexagons, as based on the Fact (2). First, we recall canonical codes [56] for primitive coronoids. Mark any arbitrary point of fusion and then in tracing along one boundary of the coronoid locate how many vertices before the next fusion, as indicated in Fig. 22. Obviously, this can be either 0, 1 or 2, whereas if traced along the other boundary of the same coronoid the respective number of carbon atoms would be 2, 1 or 0. With  $a_i$  this number of vertices for the  $i$ th hexagon, the sequence  $(a_1, a_2, \dots, a_n)$  then specifies the particular coronoid. But since any one of the hexagons might be chosen as the first, and since counts might be either to the right or to the left, and since one side of the coronoid or the other might be identified as the one to be traced along, it is seen that (up to)  $4n$  codes are conceivable. Now each of these  $4n$  (sometimes redundant) strings of digits may be viewed as a ternary number, whence from all these numbers we choose the smallest to correspond to the canonical code. This  $n$ -tuple code is a distinct identification for a particular primitive coronoid.

**Fig. 22** Canonical code

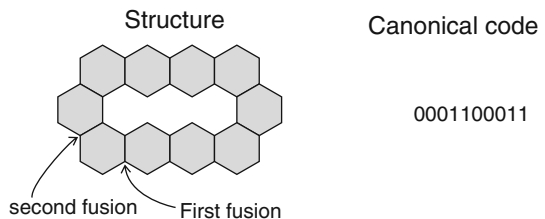


**Table 2** The canonical codes of the primitive coronoids with 10 hexagons

$n$	Code	Code	Code
1	0001100011	0010100101	0001010002

**Table 3** The canonical codes of the primitive coronoids with 11 hexagons

$n$	Code	Code
1	00101010011	00011001002

**Table 4** The canonical codes of the primitive coronoids with 12 hexagons

$n$	Code	Code	Code	Code
1	000111000111	001100110011	001011001011	000110100102
2	000101100012	010101010101	001010101002	000102000102
3	001002001002	000200101002	000200020002	

**Table 5** The canonical codes of the primitive coronoids with 13 hexagons

$n$	Code	Code	Code	Code
1	0010110100111	0011010101011	0001110010021	0001110010102
2	0010110011002	0010101100102	0001110002002	0001101010012
3	0002001100102	0001100200012	0001020010012	0010020100102

**Table 6** The canonical codes of the primitive coronoids with 14 hexagons

$n$	Code	Code	Code	Code
1	00011110001111	00110101100111	00101110010111	00110110011011
2	00102001100111	00011100110012	00011101001102	00010111000112
3	00011101001021	01010110101011	00102010011011	00011011001012
4	00011011000121	00110101011002	00011020001102	00110020011002
5	00101011010012	00101101010102	00011011000202	00010210001102
6	00020011010012	00101100200102	00102010010201	00100120010012
7	00101101002002	00010110100022	00010201001012	00100201010012
8	00012001010021	00010120001012	00101020010102	00012001010102
9	00012000200102	00020100200102	00010201000202	00012000200021
10	00012001002002	00020020010102	00020020002002	

**Remark 5** The writhe  $W(C)$  of the inner dual graph  $C$  of a coronoid depends on its canonical code in a fairly simple way:  $W(C) = \frac{n_0 - n_2}{6}$ , where  $n_0, n_2$  is the number of 0, 2 in the canonical code resp. To see this result note that as one turns in following the edges of  $C$  around  $C$  to return to the initial site, one turns through a net angle



**Table 7** The canonical codes of the primitive coronoids with 15 hexagons

<i>n</i>	Code	Code	Code	Code
1	001110011100111	001011101001111	000111100100211	000111100101102
2	001101101010111	000111100101021	001101100200111	001011100110021
3	001011100110102	010110101101011	000111100020102	000111100012002
4	001011011001102	000110110100112	001020101010111	001010111001012
5	000111010100121	001011011001021	000111010101012	001011010110012
6	001020100111002	001101011010102	000200111001012	000111002001012
7	000120011001102	001011100102002	000101110010022	000111002000121
8	000111010020012	000110021000112	000201011001102	000111010100202
9	000110102000112	001002100110012	000120011001021	001101011002002
10	000110101100022	001010200110012	001010201001102	000101200100112
11	000120100110102	001002011001012	000102010100112	000110200100121
12	000120010110012	001011002010012	000201010110012	001100201010102
13	000110200101012	000111002000202	001020011010102	001010201001021
14	001002101001021	000102100101012	000200200110012	000200201001102
15	001020011002002	000102001100022	000110200100202	000110200020012
16	000102002000112	000120100102002	000102100100202	000201002010012
17	000120002010012	000102100020012	001020010200102	000120001200012

**Table 8** The benzenoid Hopf link of type III with 22–25 hexagons

$10_1^1, 10_1^2, 10_1^3$	$12_1^2, 12_1^3, 12_1^4, 12_2^2, 12_2^3, 12_2^3$
$10_1^2$	$12_1^2, 12_1^3, 12_1^4, 12_2^2, 12_2^3, 12_3^1, 12_3^2$
$11_1^1, 11_1^2$	$11_1^1, 11_1^2$
$10_1^1, 10_1^3$	$13_1^1, 13_1^2, 13_1^3, 13_1^4, 13_2^1, 13_2^2, 13_2^3, 13_2^4, 13_3^1, 13_3^3$
$10_1^2$	$13_1^1, 13_1^2, 13_1^3, 13_1^4, 13_2^1, 13_2^2, 13_2^3, 13_2^4, 13_3^1, 13_3^2, 13_3^3, 13_3^4$
$11_1^1$	$12_1^1, 12_1^2, 12_1^3, 12_1^4, 12_2^1, 12_2^2, 12_2^3, 12_2^4, 12_3^1, 12_3^2, 12_3^3$
$11_1^2$	$12_1^2, 12_1^3, 12_1^4, 12_2^2, 12_2^3, 12_3^1, 12_3^2$
$10_1^1, 10_1^3$	$14_1^2, 14_1^3, 14_1^4, 14_2^1, 14_2^2, 14_2^3, 14_3^1, 14_3^2, 14_3^3, 14_4^1, 14_4^2, 14_4^3, 14_4^4, 14_5^1, 14_5^2, 14_5^3, 14_5^4, 14_6^1, 14_6^2, 14_6^3, 14_6^4, 14_7^1, 14_7^2, 14_7^3, 14_7^4, 14_8^1, 14_8^2, 14_8^3, 14_8^4, 14_9^1, 14_9^2, 14_9^3, 14_9^4, 14_{10}^1, 14_{10}^2, 14_{10}^3, 14_{10}^4$
$10_1^2$	$14_1^2, 14_1^3, 14_1^4, 14_2^1, 14_2^2, 14_2^3, 14_3^1, 14_3^2, 14_3^3, 14_4^1, 14_4^2, 14_4^3, 14_5^1, 14_5^2, 14_5^3, 14_6^1, 14_6^2, 14_6^3, 14_7^1, 14_7^2, 14_7^3, 14_8^1, 14_8^2, 14_8^3, 14_9^1, 14_9^2, 14_{10}^1, 14_{10}^2, 14_{10}^3, 14_{10}^4$
$11_1^1$	$13_1^1, 13_1^2, 13_1^3, 13_1^4, 13_2^1, 13_2^2, 13_2^3, 13_2^4, 13_3^1, 13_3^2, 13_3^3, 13_3^4$
$11_1^2$	$13_1^1, 13_1^2, 13_1^3, 13_1^4, 13_2^1, 13_2^2, 13_2^3, 13_2^4, 13_3^1, 13_3^2, 13_3^3, 13_3^4$
$12_1^2, 12_1^3, 12_1^4,$	
$12_2^2, 12_2^3, 12_2^3$	$12_1^1, 12_1^2, 12_1^3, 12_1^4, 12_2^1, 12_2^2, 12_2^3, 12_2^4, 12_3^1, 12_3^2, 12_3^3, 12_3^3$
$12_1^1, 12_2^1, 12_2^4, 12_3^3$	$12_1^2, 12_1^3, 12_1^4, 12_2^2, 12_2^3, 12_2^3$
$12_1^1$	$12_1^2, 12_1^3, 12_1^4, 12_2^2, 12_2^3, 12_3^1, 12_3^2$

**Table 8** continued

	$15_1^1, 15_1^2, 15_1^4, 15_2^1, 15_2^2, 15_2^3, 15_2^4, 15_3^1, 15_3^2, 15_3^3, 15_3^4, 15_4^1, 15_4^2, 15_4^3, 15_4^4, 15_5^1, 15_5^2, 15_5^3, 15_5^4, 15_6^1, 15_6^2, 15_6^3, 15_6^4, 15_7^1, 15_7^2, 15_8^1, 15_8^2, 15_8^3, 15_8^4, 15_9^1, 15_9^2, 15_9^3, 15_9^4,$
$10_1^1, 10_1^3$	$15_9^4, 15_{10}^1, 15_{10}^2, 15_{10}^3, 15_{10}^4, 15_{11}^1, 15_{11}^2, 15_{11}^3, 15_{11}^4, 15_{12}^1, 15_{12}^2, 15_{12}^3, 15_{12}^4, 15_{13}^1, 15_{13}^2, 15_{13}^3, 15_{13}^4, 15_{14}^1, 15_{14}^2, 15_{14}^3, 15_{14}^4, 15_{15}^1, 15_{15}^2, 15_{15}^3, 15_{15}^4, 15_{16}^1, 15_{16}^2, 15_{16}^3, 15_{16}^4, 15_{17}^1, 15_{17}^2, 15_{17}^3, 15_{17}^4,$
	$15_1^1, 15_1^2, 15_1^3, 15_1^4, 15_2^1, 15_2^2, 15_2^3, 15_2^4, 15_3^1, 15_3^2, 15_3^3, 15_3^4, 15_4^1, 15_4^2, 15_4^3, 15_4^4, 15_5^1, 15_5^2, 15_5^3, 15_5^4, 15_6^1, 15_6^2, 15_6^3, 15_6^4, 15_7^1, 15_7^2, 15_7^3, 15_7^4,$
$10_1^2$	$15_8^1, 15_8^2, 15_8^3, 15_8^4, 15_9^1, 15_9^2, 15_9^3, 15_9^4, 15_{10}^1, 15_{10}^2, 15_{10}^3, 15_{10}^4, 15_{11}^1, 15_{11}^2, 15_{11}^3, 15_{11}^4, 15_{12}^1, 15_{12}^2, 15_{12}^3, 15_{12}^4, 15_{13}^1, 15_{13}^2, 15_{13}^3, 15_{13}^4, 15_{14}^1, 15_{14}^2, 15_{14}^3, 15_{14}^4, 15_{15}^1, 15_{15}^2, 15_{15}^3, 15_{15}^4, 15_{16}^1, 15_{16}^2, 15_{16}^3, 15_{16}^4, 15_{17}^1, 15_{17}^2, 15_{17}^3, 15_{17}^4,$
	$14_1^1, 14_1^2, 14_1^3, 14_1^4, 14_2^1, 14_2^2, 14_2^3, 14_2^4, 14_3^1, 14_3^2, 14_3^3, 14_3^4, 14_4^1, 14_4^2, 14_4^3, 14_4^4, 14_5^1, 14_5^2, 14_5^3, 14_5^4, 14_6^1, 14_6^2, 14_6^3, 14_6^4, 14_7^1, 14_7^2, 14_7^3, 14_7^4,$
$11_1^1$	$14_8^1, 14_8^2, 14_8^3, 14_8^4, 14_9^1, 14_9^2, 14_9^3, 14_9^4, 14_{10}^1, 14_{10}^2, 14_{10}^3, 14_{10}^4, 14_{11}^1, 14_{11}^2, 14_{11}^3, 14_{11}^4, 14_{12}^1, 14_{12}^2, 14_{12}^3, 14_{12}^4, 14_{13}^1, 14_{13}^2, 14_{13}^3, 14_{13}^4, 14_{14}^1, 14_{14}^2, 14_{14}^3, 14_{14}^4,$
	$14_1^1, 14_2^1, 14_3^1, 14_4^1, 14_5^1, 14_6^1, 14_7^1, 14_8^1, 14_9^1, 14_{10}^1, 14_{11}^1, 14_{12}^1, 14_{13}^1, 14_{14}^1, 14_1^2, 14_2^2, 14_3^2, 14_4^2, 14_5^2, 14_6^2, 14_7^2, 14_8^2, 14_9^2, 14_{10}^2, 14_{11}^2, 14_{12}^2, 14_{13}^2, 14_{14}^2,$
$11_1^2$	$14_1^1, 14_2^1, 14_3^1, 14_4^1, 14_5^1, 14_6^1, 14_7^1, 14_8^1, 14_9^1, 14_{10}^1, 14_{11}^1, 14_{12}^1, 14_{13}^1, 14_{14}^1, 14_1^2, 14_2^2, 14_3^2, 14_4^2, 14_5^2, 14_6^2, 14_7^2, 14_8^2, 14_9^2, 14_{10}^2, 14_{11}^2, 14_{12}^2, 14_{13}^2, 14_{14}^2,$
	$14_1^3, 14_2^3, 14_3^3, 14_4^3, 14_5^3, 14_6^3, 14_7^3, 14_8^3, 14_9^3, 14_{10}^3, 14_{11}^3, 14_{12}^3, 14_{13}^3, 14_{14}^3, 14_1^4, 14_2^4, 14_3^4, 14_4^4, 14_5^4, 14_6^4, 14_7^4, 14_8^4, 14_9^4, 14_{10}^4, 14_{11}^4, 14_{12}^4, 14_{13}^4, 14_{14}^4,$
$12_1^1, 12_2^4, 12_2^1$	$13_1^1, 13_1^2, 13_1^3, 13_1^4, 13_2^1, 13_2^2, 13_2^3, 13_2^4, 13_3^1, 13_3^2, 13_3^3, 13_3^4$
$12_2^1, 12_4^4, 12_3^3$	
$12_2^2, 12_3^3, 12_3^2$	$13_1^1, 13_1^2, 13_1^3, 13_1^4, 13_2^1, 13_2^2, 13_2^3, 13_2^4, 13_3^1, 13_3^2, 13_3^3, 13_3^4$
$12_3^1$	$13_1^1, 13_1^2, 13_1^3, 13_1^4, 13_2^1, 13_2^2, 13_2^3, 13_2^4, 13_3^1, 13_3^2, 13_3^3, 13_3^4$
$12_3^3$	$13_1^1, 13_1^2, 13_1^3, 13_1^4, 13_2^1, 13_2^2, 13_2^3, 13_2^4, 13_3^1, 13_3^2, 13_3^3, 13_3^4$

of  $W(C) \times 360^\circ$ . Concretely when we turn at a vertex  $v_i$ , we turn  $60^\circ$ ,  $0$  or  $-60^\circ$  depending on  $a_i$  of the canonical code.

Let  $15_m^n$  ( $10_m^n$ ,  $11_m^n$ ,  $12_m^n$ ,  $13_m^n$ ,  $14_m^n$ , resp.) denote the primitive coronoid in the  $(m + 1)$ -th row and  $(n + 1)$ -th column of Table 7 (2, 3, 4, 5, 6, resp.). We list all the benzenoid Hopf link of type III with 22–25 hexagons in Table 8. Each of them is made by two primitive coronoids in the same row, such that one is from the first column, the other is from the second column.

## References

1. D.S. Silver, Knot theory's odd origins. *Am. Sci.* **44**, 158–165 (2006)
2. L.H. Kauffman, *Knots and Physics* (World Scientific Publishing Co., Singapore, 2001)
3. L.F. Liu, R.E. Depew, J.C. Wang, Knotted single-stranded DNA rings: a novel topological isomer of circular single-stranded DNA formed by treatment with Escherichia coli omega protein. *J. Mol. Biol.* **106**(2), 439–452 (1976)
4. D.W.L. Summers, Knot theory and DNA, *proc. Symp. Appl. Math.* **45**, 39–72 (1992)
5. A.D. Bates, A. Maxwell, *DNA Topology* (Oxford University Press, Oxford, 1993)
6. C. Liang, K. Mislow, Knots in proteins. *J. Am. Chem. Soc.* **116**, 11189–11190 (1994)
7. W.R. Taylor, A deeply knotted protein structure and how it might fold. *Nature* **406**, 916–919 (2000)
8. H.L. Frisch, E. Wassermann, Chemical topology. *J. Am. Chem. Soc.* **83**, 3789–3795 (1961)
9. M. Delbruck, *Proc. Symp. Appl. Math.* **14**, 55 (1962)

10. M.D. Frank-Kamenetskii, A.V. Lukashin, Statistical mechanics and topology of polymer chains, A.V. Vologodskii, *Nature* **258**, 398 (1975)
11. C.O. Dietrich-Buchecker, J.P. Sauvage, A synthetic molecular trefoil knot. *Angew. Chem. Int. Ed.* **28**, 189 (1989)
12. F.M. Raymo, J.F. Stoddart, Interlocked macromolecules. *Chem. Rev.* **99**, 1643–1663 (1999)
13. B.F. Hoskins, R. Robson, Design and construction of a new class of scaffolding-like materials comprising infinite polymeric frameworks of 3D-linked molecular rods. *J. Am. Chem. Soc.* **112**, 1546–1554 (1990)
14. H.S. Zhadanov, *C. Rend. Acad. Sci. URSS* **31**, 350–354 (1941)
15. J. Konnert, D. Britton, The crystal structure of  $\text{AgC}(\text{CN})_3$  *inorg. Chem.* **5**, 1193–1196 (1966)
16. H. Adams et al., Knot tied around an octahedral metal centre. *Nature* **411**, 763 (2001)
17. O. Lukin et al., Knotaxanes–Rotaxanes with knots as stoppers. *Angew. Chem. Int. Ed.* **42**, 4542–4545 (2003)
18. O. Lukin et al., Topologically chiral covalent assemblies of molecular knots with linear, branched, and cyclic architectures. *Chem. Eur. J.* **10**, 2804–2810 (2004)
19. V. Balzani et al., Artificial molecular machines, *angew. Chem. Int. Ed.* **39**, 3348–3391 (2000)
20. E. Flappan, *When Topology Meets Chemistry* (Cambridge University Press, Cambridge, 2000)
21. M. Deza, M. Dutour, P.W. Fowler, Zigzags, railroads, and knots in fullerenes. *J. Chem. Inf. Comput. Sci.* **44**, 1282–1293 (2004)
22. P.G. Mezey, Tying knots around chiral centers: chirality polynomials and conformational invariants for molecules. *J. Am. Chem. Soc.* **108**, 3976–3984 (1986)
23. E. Clar, *Polycyclic Hydrocarbons, Vol. I–II* (Academic Press, London, 1964)
24. A.T. Balaban, M. Banciu, V. Ciorba, *Annulenes, Benzo-, Hetero-, Homo-, Derivatives, and their Valence Isomers, Volumes I–III* (CRC, Boca-Raton, 1987)
25. S.J. Cyvin, I. Gutman, *Kekule Structures in benzenoid Hydrocarbons* (Springer-verlag, Berlin, 1988)
26. I. Gutman, S.J. Cyvin, *Introduction to the Theory of Benzenoid Hydrocarbons* (Springer-verlag, Berlin, 1989)
27. R.G. Harvey, *Polycyclic Aromatic Hydrocarbons* (Wiley-VCH, New York, 1997)
28. H. Hopf, *Classics in Hydrocarbon Chemistry* (Wiley-VCH, Weinheim, 2000)
29. D. Astruc (ed.), *Modern Arene Chemistry* (Wiley-VCH, Weinheim, 2002)
30. F. Diederich, H.A. Staab, Benzenoid versus annulenic aromaticity synthesis and properties of kekulene. *Angew. Chem. Int. Ed. Engl.* **17**, 372 (1978)
31. C. Krieger et al., Molecular structure and spectroscopic properties of kekulene. *Angew. Chem. Int. Ed. Engl.* **18**, 699 (1979)
32. C. Schweitzer et al., Electronic properties of kekulene. *Mol. Phys.* **46**, 1141 (1982)
33. H.A. Staab, F. Diederich, cycloarenes, a new class of aromatic compounds—I—synthesis of kekulene. *Chem. Ber.* **116**, 3487 (1983)
34. H.A. Staab et al., cycloarenes, a new class of aromatic compounds—II—molecular structure and spectroscopic properties of kekulene. *Chem. Ber.* **116**, 3504 (1983)
35. H.A. Staab et al., cycloarenes, a new class of aromatic compounds—III—studies towards the synthesis of cyclo [d.e.d.e.e.d.e.d.e] decakisbenzene. *Chem. Ber.* **116**, 2262 (1983)
36. G. Ege, H. Fischer, Zuer konjugation in makrocyclischen bindungs-system-VI—SCF-MO-Berechnung der Bindungsabstände in makrocyclischen Bindungssystemen. *Tetrahedron* **23**, 149 (1967)
37. G. Ege, H. Fischer, Zuer konjugation in makrocyclischen Bindungs-system XX-Charakterordnung, magnetische Suszeptibilitäten und chemische Verschiebungen von Corannulenen. *Theor. Chim. Acta* **26**, 55 (1972a)
38. H. Vogler, Calculation of H-chemical shifts of kekulene and similar compounds. *Tetrahedron Lett.* **20**, 229 (1979)
39. H. Vogler, Zero-field splitting parameters D of macrocyclic systems. *Croat. Chem. Acta* **53**, 667 (1980)
40. H. Vogler, Theoretical study of geometries and  $^1\text{H}$ -chemical shifts of cycloarenes. *J. Mol. Struct. (Theochem)* **122**, 333 (1985)
41. M. Randić, On the role of kekulene valence structures. *Pure Appl. Chem.* **55**, 347 (1983)
42. S.J. Cyvin et al., Kekule structure counts: general formulations for primitive coronoid hydrocarbons. *Monatsh Chem.* **122**, 435 (1991)
43. F.J. Zhang, S.J. Cyvin, B.N. Cyvin, “Crowns”, and aromatic sextets in primitive coronoid hydrocarbons. *Monatsh Chem.* **121**, 421 (1990)

44. F.J. Zhang, M.L. Zheng, Generalized hexagonal systems with each hexagon being resonant. *Discrete Appl. Math.* **36**, 67 (1992)
45. F.J. Zhang, R.S. Chem, S.J. Cyvin, A complete solution of Hosoya's mystery. *Acta. Math. Appl. Sinica.* **12**, 263–271 (1996)
46. B.N. Cyvin, J. Brunvoll, in *Enumeration of benzenoid systems and other polyhexes*, ed. by I. Gutman, S.J. Cyvin *Advances in the Theory of Benzenoid Hydrocarbons II*, Topics in Current Chemistry, vol 162 (Springer-Verlag, Berlin, 1992b), p. 65
47. S.J. Cyvin, J. Brunvoll, B.N. Cyvin, *Theory of Coronoid Hydrocarbons. Lecture Notes Chem.*, vol. 54 (Springer-Verlag, Berlin, 1991)
48. S.J. Cyvin, J. Brunvoll, R.S. Chem, B.N. Cyvin, F.J. Zhang, *Theory of Coronoid Hydrocarbons II. Lecture Notes Chem.*, vol. 62 (Springer-Verlag, Berlin, 1994)
49. M.S. Newman, D. Lednicer, The synthesis and resolution of hexahelicene. *J. Am. Chem. Soc.* **78**, 4765 (1956)
50. B.N. Cyvin, X.F. Guo, S.J. Cyvin, F.J. Zhang, Enumeration of helicenes. *Chem. Phys. Lett.* **188**, 537 (1992)
51. S.J. Cyvin, B.N. Cyvin, Theory of helicenic hydrocarbons-part 2- chemical formulas. *Struct. Chem.* **4**, 303 (1993)
52. S.J. Cyvin, F.J. Zhang, B.N. Cyvin, X.F. Guo, Theory of helicenic hydrocarbons-part 1- invariants and symmetry. *Struct. Chem.* **4**, 149 (1993)
53. M. Flammang-barbieux, J. Nasielski, R.H. Martin, Synthesis of heptahelicene (1) benzo [c] phenanthro[4,3-g] phenanthrene. *Tetrahedron* **8**(8), 743–744 (1967)
54. R.H. Martin et al, 1-synthesis of octa- and nonahelicenes. 2- new syntheses of hexa- and heptahelicenes. 3- optical rotation and O.R.D of heptahelicene. *Tetrahedron* **9**(31), 507–3510 (1968)
55. P.L. Pauson, B.J. Williams, Cyclopentadienes, fulvenes, and fulvalenes, Part I. A hexapheny fulvalene. *J. Chem. Soc.* 4153–4157 (1961)
56. A. Misra, D.J. Klein, Characterization of cyclo-polyphenacenes. *J. Chem. Inf. Comput. Sci.* **42**, 1171–1175 (2002)
57. J.Cz. Dobrowolski, On the belt and moebius isomers of the coronene molecule. *J. Chem. Inf. Comput. Sci.* **42**, 490–499 (2002)
58. L. Wang, F. Zhang, H. Zhao, On the ordering of benzenoid chains and cyclo-polyphenacenes with respect to their numbers of clar aromatic sextets. *J. Math. Chem.* **38**(2), 293–309 (2005)
59. D.J. Klein, A. Misra, Topological isomer generation & enumeration: application for polyphenacenes. *Commun. Math. Comp. Chem. (MatCh)* **46**, 45–69 (2002)
60. Y. Fujioka, Syntheses and physical properties of several polyphenylenes containin mixed linkages. *Bull. Chem. Soc. Jpn.* **57**, 3494–3506 (1984)